Transactions of the KSNVE, Vol. 14, No. 5, pp. 416~423, 2004.

System Identification of a Three-story Test Structure based on Finite Element Model

유한요소모델에 기초한 3층 건물모델의 시스템 식별

Kyung-Soo Kang, Sang-Hyun Lee and Kyung-Won Min

강 경 수† · 이 상 현* · 민 경 원**

(Received January 29, 2004 : Accepted April 7, 2004)

Key Words : System Identification(시스템식별), Finite Element Model(유한요소모델), Active Mass Driver(능동질량감쇠기)

ABSTRACT

In this paper, an experimental verification of system identification technique for constructing finite element model is conducted for a three-story test structure equipped with an active mass driver (AMD). Twenty Gaussian white noises were used as the input for AMD, and the corresponding accelerations of each floor are measured. Then, the complex frequency response function (FRF) for the input, the force induced by the AMD, was obtained and subsequently, the Markov parameters and system matrices were estimated. The magnitudes as well as phase of experimentally obtained FRFs match well with those of analytically obtained FRFs.

요 약

본 연구에서는, 능동질량감쇠기가 설치된 3층 건물 축소 실험을 통해 유한요소모델에 기초한 시스템 식별기법의 유효성을 검증하였다. 입력 신호로는 능동질량감쇠기를 통해 구현되는 20개의 가우시안 백색잡음을 사용하였으며, 출력 신호로는 각층에 설치된 가속도계를 사용하여 측정된 각층 절대가속도를 사용하였다. 복소진동수응답함수를 구성한 후, 마코프(Markov) 파라메터와 시스템 행렬을 추출하였으며, 이로부터 CBSI기법을 이용하여 유한요소모델을 식별하였다. 식별된 유한요소모델과 실험을 통해 얻어진 복소응답함수는 매우 일치함을 확인할 수 있었다.

1. Introduction

In recent years, researches have been extensively carried out analytically and experimentally on the active control of civil engineering structures subjected to earthquake and wind loads.[1~2] Generally, the accurate modeling of the structure is required in active control in order to achieve stability and desired control performance. Accordingly, various system identification methods have been utilized for the accurate modeling of the structure.[3~4] In special, most of experimental research on active control relies on the accurate system identification, and the control performances of adopted control algorithms are guaranteed by the accurate

† 책임저자 : 정회원, 동명정보대학교 건축공학과
E-mail : koosin@tit.ac.kr
Tel : (051) 610-8604, FAX : (051) 610-8840
* 서울대학교 공학연구소 객원연구원, 공학박사
** 정회원, 단국대학교 건축공학과 부교수

estimation of test models.[5~8]

For design of control systems in active control of structures under seismic loads, two separate system matrices are first identified for two input signals earthquakeload and active control force and then condensed into an integrated system matrix.[9~10] This procedure, however, is only applicable for small-sized structures which are suitable for the shaking table test. It is almost impossible to apply seismic forces to real civil structures for system identification purpose.

In general, the mass, damping, and stiffness of civil structures are modeled using the finite element method (FEM). The FEM model has an advantage that earthquake loads are easily modeled. However, the FEM model may show a large discrepancy with the actual structure in terms of dynamic characteristics due to uncertainties includedin modeling. In this case, it is required to refine the FEM model applying system identification techniques in order to guarantee the desired performance of control system.[11~12] Otherwise, a new control algorithm, which shows a robust control performance in spite of the uncertainties in FEM modeling, needs to be developed.

In this paper, an experimental verification of system identification technique for constructing second-order system is conducted for a three-story test structure equipped with an active mass driver (AMD). All of acceleration information of AMD, shaking table, and three floors are used for the system identification.

2. Experimental Setup

Experimental investigations were performedin the Structural Lab at Seoul National University, Seoul, Korea. The test structure used in this experiment was a three-story, single-bay, steel frame shown in Fig. 1. The height and width of the structure were 120 cm and 60 cm, respectively. Shevron braces were used to stiffen the test structure so that its behavior in moving direction governed. The structure was excited by a uniaxial shaking table on which it was mounted. The shaking table used an AC servomotor and its

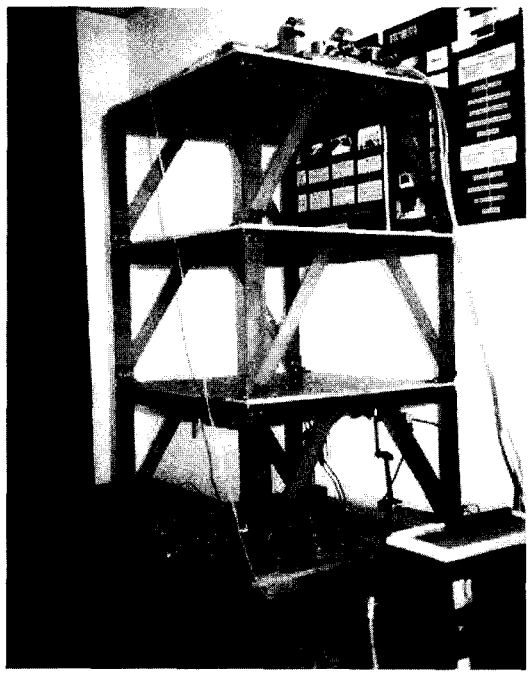

Fig. 1 Test Structure with AMD system

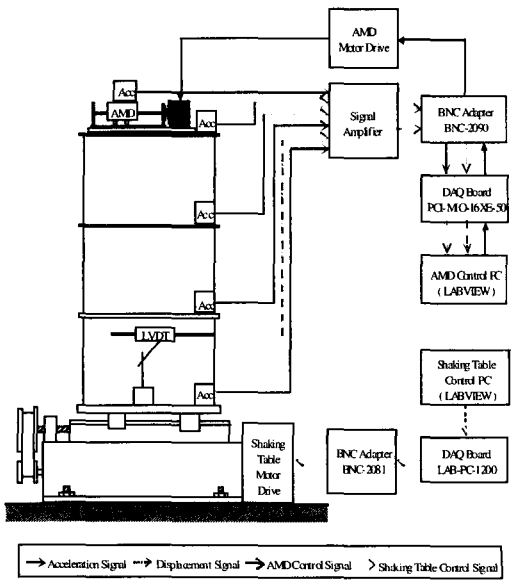

Fig. 2 Schematic diagram of experimental setup

movement was controlled by a separate computer through a National Instrument (NI) LAB-PC-1200 D/A board and an NI BNC-2081 board.

The control force was supplied by an AMD attached to the top floor of the test structure. The AMD was comprised of a moving mass of 4.7 kg, a ball screw unit, and an AC servomotor. The maximum stroke of the AMD was 150 mm with the maximum acceleration generating capacity of 500 cm/sec^2.

The accelerometers were positioned on each floor of the structureto measure the absolute accelerations of the test structure. Additionally, accelerometers located on the AMD and on the base measured the absolute accelerations of the AMD and the ground excitation. A linear variable differential transformer (LVDT) displacement transducer was installed on the first floor to measure the floor displacement. The data acquisition and implementation of the digital controller were performed using a real-time digital signal processor (DSP). The primary tasks of the data acquisition board were to perform the analog to digital (A/D) conversion of the measured acceleration data, and to perform the digital to analog (D/A) conversion of the command signal computed by the control program. A 16-channel data acquisition system was employed using a NI PCI-MIO-16XE-50 board and a NI BNC-2090 board. The schematic of the entire test system is presented in Fig. 2.

3. System Identification

It is critical to develop an accurate analytical model of the structure in the experimental verification of control systems.[5] In general, the steps involved in the experiment on a control system are (1) establishing an exact model of test structure applying the system identification techniques, (2) designing a control system based on the identified model, and (3) experimental verification of the control system. In this chapter, a FEM model of the test structureis derived in terms of mass, damping, and stiffness, and a comparison of the experimental and analytical transfer functions is performed to verify the accuracy of the obtained model. This FEM model will serve as a basis model for the robustness verification of the proposed probabilistic control algorithm against the modeling uncertainties in the subsequent sections.

In this study, system identification for the test structure and control system was performed in the frequency-domain. The system inputs were the accelerations of the AMD, and the system outputs were the absolute accelerations of three floors. The steps involved in the system identification procedure included (1) obtaining a complex frequencyresponse function (FRF) using the system inputs and outputs; (2) estimating the system Markov parameters from the FRF; (3) minimum realization of the system obtaining a state-space model from the Markov parameters; and (4) obtaining the modal properties from the state-space model and constructing the analytical FEM model.

3.1 Complex Frequency Response Function

Consider a discrete multivariable linear system described by

$$\boldsymbol{z}(k+1) = \boldsymbol{A}_d \boldsymbol{z}(k) + \boldsymbol{B}_d \boldsymbol{u}(k) \tag{1-a}$$

$$\boldsymbol{y}(k) = \boldsymbol{C}_d \boldsymbol{z}(k) + \boldsymbol{D}_d \boldsymbol{u}(k) \tag{1-b}$$

where $z(k)$ is an $(n\times1)$ state vector, $y(k)$ is an $(m\times1)$ system output vector, and $u(k)$ is an $(r\times1)$ system input vector for $k = 0, \cdots, l\text{-}1$ with A_d, B_d, C_d, and D_d being system matrices with appropriate dimensions. The relationship between $u(t)$ and $y(t)$ can be expressed as follows assuming zero initial conditions.[3]

$$\boldsymbol{y}(k) = \sum_{\tau=0}^{\infty} \boldsymbol{Y}_\tau \boldsymbol{u}(k-\tau) \tag{2}$$

where $Y_\tau(\tau = 1, \cdots, \infty)$ is the system Markov parameters to be determined. Applying the discrete Fourier transform (DFT) to Eq. (3) yields

$$\boldsymbol{Y}(k) = \boldsymbol{G}(z_k)\boldsymbol{U}(k) \tag{3}$$

where $Y(k)$ and $U(k)$ are Fourier transforms of $y(k)$ and $u(k)$, respectively, and

$$\boldsymbol{G}(z_k) = \sum_{\tau=0}^{\infty} \boldsymbol{Y}_\tau e^{-j\frac{2\pi k}{l}\tau} \qquad z_k = e^{-j\frac{2\pi k}{l}} \tag{4}$$

in which the matrix $G(z_k)$ is the complex FRF for the frequency at $2\pi k/l$, z_k is the z-transform variable, and $j=\sqrt{-1}$. For multi-input multi-output (MIMO) systems, in general, the complex FRF is obtained from N experiments or N data segments of a long experiment record. For N input-output relationships, post-multiplying both sides of Eq. (4) by $U^*(k)$, which is the complex conjugate transpose of $U(k)$, produces

$$\sum_{i=1}^{N} \boldsymbol{Y}^{(i)}(k)\boldsymbol{U}^{(i)*}(k) = \boldsymbol{G}(z_k)\sum_{i=1}^{N} \boldsymbol{U}^{(i)}(k)\boldsymbol{U}^{(i)*}(k) \tag{5}$$

where $U^{(i)}(k)$ and $Y^{(i)}(k)$, respectively, represent the DFTs of the input sequence, $u(k)$, and output sequence, $y(k)$, for i-th data ($i = 1, \cdots, N$). Then, the complex FRF is calculated as

$$\boldsymbol{G}(z_k) = \sum_{i=1}^{N} \boldsymbol{Y}^{(i)}(k)\boldsymbol{U}^{(i)*}(k)\left[\sum_{i=1}^{N} \boldsymbol{U}^{(i)}(k)\boldsymbol{U}^{(i)*}(k)\right]^{-1} \tag{6}$$

3.2 System Markov Parameters

To obtain the system Markov parameters, which represent a pulse response of the system, we first decompose the complex FRF using the left matrix fraction method as[3]

$$\boldsymbol{G}(z_k) = \overline{\boldsymbol{Q}}(z_k)^{-1}\overline{\boldsymbol{R}}(z_k) \tag{7}$$

where matrix polynomials $\overline{\boldsymbol{Q}}(z_k)$ and $\overline{\boldsymbol{R}}(z_k)$ are

$$\overline{\boldsymbol{Q}}(z_k) = \boldsymbol{I}_m + \overline{\boldsymbol{Q}}_1 z_k^{-1} + \cdots + \overline{\boldsymbol{Q}}_p z_k^{-p} \tag{8}$$

$$\overline{\boldsymbol{R}}(z_k) = \overline{\boldsymbol{R}}_0 + \overline{\boldsymbol{R}}_1 z_k^{-1} + \cdots + \overline{\boldsymbol{R}}_p z_k^{-p} \tag{9}$$

assuming the orders of both polynomials to be p and I_m is an identity matrix of order m. $\overline{\boldsymbol{Q}}_i$ ($i = 1, \cdots, p$) is an $m \times m$ real matrix and $\overline{\boldsymbol{R}}_i$ ($i = 1, \cdots, p$) is an $m \times r$ real matrix. Pre-multiplying Eq. (7) by $\overline{\boldsymbol{Q}}(z_k)$ and rearranging terms of like powers lead to

$$\boldsymbol{Y}_0 = \boldsymbol{D}_d = \overline{\boldsymbol{R}}_0 \tag{10}$$

$$\boldsymbol{Y}_\tau = \overline{\boldsymbol{R}}_\tau - \sum_{i=1}^{\tau} \overline{\boldsymbol{Q}}_i \boldsymbol{Y}_{\tau-i} \quad \text{for } = 1, \cdots, p \tag{11}$$

$$\boldsymbol{Y}_\tau = -\sum_{i=1}^{p} \overline{\boldsymbol{Q}}_i \boldsymbol{Y}_{\tau-i} \quad \text{for } = p+1, \cdots, \infty \tag{12}$$

3.3 Minimum Realization

A realization of the system is to obtain the system matrices, A_d, B_d, and C_d, which satisfy the discrete equation of motion for the system, from the Markov parameters, Y_τ ($\tau = 1, \cdots, \infty$), presented in Eqs. (10) to (12). Any system has an infinite number of realizations which will predict the identical response subjected to a specific input. The minimum realization means to obtain a state-space model with the smalleststate-space dimension among the infinite realizable systems, which represent the same input-output relationship. In this study, the Eigensystem Realization Algorithm method with Data Correlation (ERA/DC) is applied to estimate the system matrices from the Markov parameters. ERA/DC is a least-square fit to the output auto-correlationsand cross-correlations over a defined number of lag values. Applying ERA/DC, the realization, $\hat{\boldsymbol{A}}$, $\hat{\boldsymbol{B}}$, and $\hat{\boldsymbol{C}}$, of system matrices,

Ad, Bd, and Cd are[3]

$$\hat{A} = \Sigma_n^{-1/2} R_n^T H(1) S_n \Sigma_n^{-1/2} \tag{13}$$

$$\hat{B} = \left[E_\gamma^T R_n \Sigma_n^{1/2}\right]^\dagger H(0) E_r \tag{14}$$

and

$$\hat{C} = E_m^T R_n \Sigma_n^{1/2} \tag{15}$$

where the superscript † denotes a pseudo-inverse, $E_\gamma = [\, I_\gamma \;\; O_\gamma \cdots O_\gamma]^T$ with a null matrix O_γ of order γ, and $H(k)$ is the block correlation Henkel matrix and is factorized using singular value decomposition for $k = 0$ such that

$$H(0) = R \Sigma S^T$$

in which the columns of matrices R and S are orthogonal, i.e., $R^T R = I$ (= identity matrix) and $S^T S = I$, and Σ is a rectangular matrix defined as

$$\Sigma = \begin{bmatrix} \Sigma_n & 0 \\ 0^T & 0 \end{bmatrix} \tag{16}$$

with

$$\Sigma_n = \mathrm{diag}(\sigma_1, \sigma_2, \cdots, \sigma_n) \tag{17}$$

where 0 is a ($n \times 1$) null vector and σ_i ($i = 1, \cdots, n$) is monotonically decreasing constants.

Transforming the above discretized state-space matrices into the continuous state-space form, we obtain

$$\dot{z} = A_c z + B_c u \tag{18}$$

$$y = C_c z + D_c u \tag{19}$$

4. FEM Model

An n-degree-of-freedom (DOF) second order system subjected to a control force u is given by

$$M\ddot{x} + C\dot{x} + Kx = bu \tag{20}$$

where M, C, and K are, respectively, the mass, damping, and stiffness matrices of size $n \times n$, and x is the displacement response vector of size $n \times 1$, and b is the control force influence matrix. Applying modal transformation, Eq. (20) can be expressed as

$$\ddot{\eta} + \Lambda\dot{\eta} + \Omega\eta = \Phi^T bu \tag{21}$$

where $x = \Phi_\eta$, Φ is the eigenvector satisfying the following characteristic equation

$$K\Phi = M\Phi\Omega \tag{22}$$

$$\Phi^T M \Phi = I \tag{23}$$

and Λ and Ω, respectively, are

$$\Omega = \Phi^T K \Phi = \mathrm{diag}(\omega_{ni}^2, i = 1, \ldots, n) \tag{24}$$

$$\Lambda = \Phi^T C \Phi = \mathrm{diag}(2\xi_i \omega_{ni}, i = 1, \ldots, n) \tag{25}$$

in which ω_{ni} and ζ_i are natural frequency and damping ratio of i th mode, respectively.

The acceleration responses of the structure in Eq. (20) are then calculated using modal coordinates, η, as

$$\ddot{x} = \Phi\ddot{\eta} = -\Phi\Omega\eta - \Phi\Lambda\dot{\eta} + bu \tag{26}$$

and the state-space equations in Eqs. (18) and (19) are transformed into the following complex modal equations.

$$\dot{q} = A_q q + B_q u \tag{27}$$

$$y = C_q q + D_c u \tag{28}$$

in which $z = \Psi q$, $B_q = \Psi^{-1} B_c$, and $C_q = C_c \Psi$ where Ψ is the eigenvalue matrix that satisfies the following characteristic equation of A_c.

$$A_c \Psi = \Psi A_q \tag{29}$$

and matrices A_q, B_q, and C_q, and vector q are

$$A_q = \begin{bmatrix} \lambda_1 & & & \\ & \bar{\lambda}_1 & & \\ & & \ddots & \\ & & & \lambda_n \\ & & & & \bar{\lambda}_n \end{bmatrix}, \quad B_q = \begin{bmatrix} b_{q1} \\ \bar{b}_{q1} \\ \vdots \\ b_{qn} \\ \bar{b}_{qn} \end{bmatrix},$$

$$C_q^T = \begin{bmatrix} c_{q1}^T \\ \bar{c}_{q1}^T \\ \vdots \\ c_{qn}^T \\ \bar{c}_{qn}^T \end{bmatrix}, \quad q = \begin{bmatrix} q_1 \\ \bar{q}_1 \\ \vdots \\ q_n \\ \bar{q}_n \end{bmatrix} \tag{30}$$

where $\lambda_i = \sigma_i + j\omega_i$ and $\bar{\lambda}_i$ is the complex conjugate of λ_i. The variable q in Eq. (30) in the complex coordinate system possesses no physical implication. By applying the common basis-normalized structural identification (CBSI) method of Alvin et al.[11], the variable q can be transformed into the modal displacement velocity model, which has the physical meaning. The following transformation is used for the coordinate transformation in CBSI.

$$\begin{bmatrix} q_i \\ \bar{q}_i \end{bmatrix} = V_i \begin{bmatrix} \eta_i \\ \dot{\eta}_i \end{bmatrix} \tag{31}$$

where the transformation matrix V_i is given as

$$V_i = d_i \frac{j}{2\omega_i} \begin{bmatrix} \sigma_i - j\omega_i & -1 \\ -\sigma_i - j\omega & 1 \end{bmatrix} \begin{bmatrix} -\sigma_i - r_i\omega_i & 1 \\ -\sigma^2{}_i - \omega_i^2 & \sigma_i - r_i \end{bmatrix} \tag{32}$$

in which $r_i = \mathrm{Im}(b_i)/\mathrm{Re}(b_i)$. d_i may be selected arbitrarily but the corresponding mode shapes are not mass-normalized ones. If a sensor is located at the same place as the actuator, mode shapes can be converted into mass-normalized ones by setting d_i as follows.

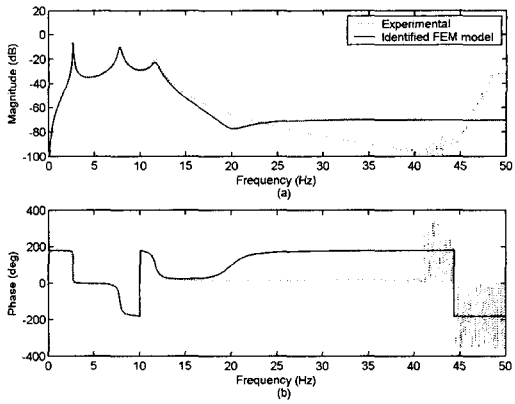

Fig. 3 Comparison of the FRFs from the input force of AMD to the absolute acceleration of the first floor

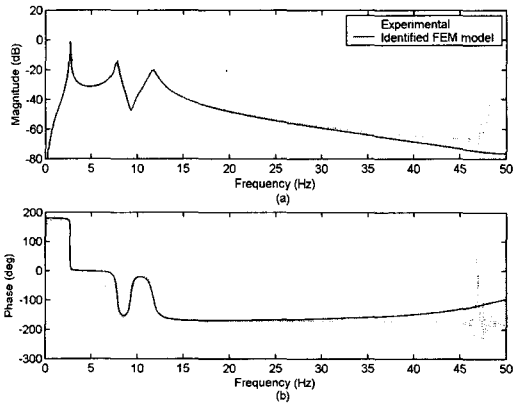

Fig. 4 Comparison of the FRFs from the input force of AMD to the absolute acceleration of the second floor

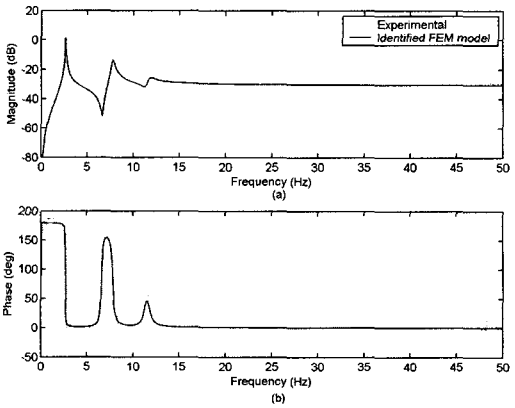

Fig. 5 Comparison of the FRFs from the input force of AMD to the absolute acceleration of the third floor

$$d_i = \omega_{ni}\sqrt{\frac{2\,\mathrm{Re}(b_i)}{(\sigma_i + r_i\omega_i)\,\mathrm{Re}(c_i) - (r_i\sigma_i - \omega_i)\,\mathrm{Im}(c_i)}} \tag{33}$$

If transforming Eq. (28) applying the transformation matrix V_i in Eq. (32) results in

$$\boldsymbol{y} = \boldsymbol{H}_1\boldsymbol{\eta} + \boldsymbol{H}_2\dot{\boldsymbol{\eta}} + \boldsymbol{D}_c\boldsymbol{u} \tag{34}$$

then, mode shapes can be obtained from Eqs. (26) and (34) such that

$$\boldsymbol{\Phi} = -\boldsymbol{H}_1\boldsymbol{\Omega}^{-1} \tag{35}$$

Using the mode shapes obtained in Eq. (35), the following mass matrix can be calculated.

$$M = (\Phi\Phi^T)^{-1} \tag{36}$$

and the stiffness matrix of the structure, K, is obtained as[11]

$$K = M\Phi\Omega\Phi^T M \tag{37}$$

Similarly, the damping matrix, C, isexpressed as

$$C = M\Phi\Lambda\Phi^T M \tag{38}$$

5. Identification Result

Twenty Gaussian white noises (N= 20) were used as the input for AMD, and the corresponding accelerations of each floors are measured. Then, the complex FRF for the input, the force induced by the AMD, was obtained and subsequently, the Markov parameters and system matrices were estimated. System matrices and corresponding analytical model are listed in Appendix I.

The FRFs of the analytically estimated model are compared with the experimentally obtained ones in Figs. 3, 4 and 5 show the FRFs from the input force of AMD to the absolute acceleration of the first, second, and third floors, respectively. Note that the experimentally obtained FRFs in the figures are the averaged ones for twenty inputs. In Fig. 3, 4 and 5, it is observed that magnitudes as well as phase of experimentally obtained FRFs match well with those of analytically obtained FRFs. Also, the FRF obtained by the third floor acceleration agrees most exactly with the experimental results. This is because the input force is directly exerted to the third floor. However, since the other FRFs provide almost exact results in the frequency range which include the natural frequencies of the structure, they can be used without much error as system model. The natural frequencies and damping ratios for the first three modes are, respectively, 2.67, 7.78 and 11.68 Hz and 0.67, 2.08 and 3.28 %.

6. Conclusion

In this paper, an experimental verification of system identification technique for constructing finite element model is conducted for a three-story test structure equipped with an active mass driver (AMD). Twenty Gaussian white noises were used as the input for AMD, and the corresponding accelerations of each floors are measured. Then, the complex FRF for the input, the force induced by the AMD, was obtained and subsequently, the Markov parameters and system matrices were estimated. The magnitudes as well as phase of experimentally obtained FRFs match well with those of analytically obtained FRFs.

Acknowledgement

The work presented in this paper was partially supported by Research Funds of the National Research Laboratory Program(Project No. M1-0203-00-0068) from the Ministry of Science and Technology in Korea.

References

(1) Housner, G.W., Bergman, L.A., Caughey,

T.K., Chassiakos, A.G., Claus, R.O., Masri, S. F. and Skelton, R.E., Soong, T.T., Spencer Jr., B. F. and Yao, J.T.P., 1997, "Special Issue Structural Control: Past, Present, and Future, Journal of Engineering Mechanics", ASCE, Vol.123, pp. 897~971.

(2) Reinhorn, A.M., Soong, T.T., Lin, R.C., Riley, M.A., Wang, Y.P., Aizawa, S. and Higashino, M., 1992, Active Bracing System: A Full Scale Implementation of Active Control, Technical Report NCEER-92-0020, State University of New York at Buffalo, Buffalo, NY.

(3) Juang, J.N., 1994, Applied System Identification, Prentice Hall, Englewood Cliffs, NJ.

(4) Ljung, L., 1987, System Identification: Theory for the User, Prentice Hall, Englewood Cliffs, NJ.

(5) Battaini, M., Yang, G. and Sepncer, Jr., B.F., 2000, "Bench-scale Experiment for Structural Control," Journal of Engineering Mechanics, Vol. 126, pp. 140~148.

(6) Spencer Jr., B.F., Dyke, S.J. and Deoskar, H.S., 1998, "Benchmark Problems in Structural Control: Part I-active mass Driver System," Earthquake Engineering and Structural Dynamics, Vol. 27, pp. 1125~1139.

(7) Chung, L.L., Lin, R.C., Soong, T.T. and Reinhorn, A. M., 1989, "Experimental Study of Active Control for MDOF Seismic Structures," Journal of Engineering Mechanics. ASCE, Vol. 115,.

(8) Hwang, J.S., 1998, Experimental Study on the Active Control of Building Structure, Ph.D. thesis (in Korean), Seoul National University, Seoul.

(9) Dyke, S.J., Spencer Jr., B.F., Quast, P., Sain, M.K., Kaspari Jr., D.C. and Soong, T.T., 1994, Experimental Verification of Acceleration Feedback Control Strategies for an Active Tendon System, Technical Report NCEER-94-0024, State University of New York at Buffalo, Buffalo, NY.

(10) Green, M. and Limebeer, D.J.N., 1995, Linear Robust Control, Prentice-Hall, Englewood Cliffs, NJ.

(11) Friswell, M.I. and Mottershead, J. E., 1995, Finite Element Model Updating in Structural Dynamics, Kluwer Academic Publishers, Boston, London,.

(12) Alvin, K.F. and Park, K.C., 1994, "Second-order Structural Identification Procedure via State-space-based System Identification," AIAA Journal, Vol. 32, pp. 397~406.

Appendix I

Identified system matrices and the corresponding FEM model properties

$$A_c=\begin{bmatrix} -0.066 & -18.416 & 0.087 & 0.035 & 0.000 & -0.027 \\ 15.281 & -0.161 & -0.004 & 0.741 & -0.105 & -0.137 \\ -0.031 & 0.216 & -0.716 & -50.035 & -0.073 & -0.025 \\ 0.078 & -0.182 & 47.773 & -1.318 & 0.070 & -0.015 \\ -0.065 & -0.127 & 0.538 & -1.242 & -2.072 & -74.159 \\ -0.068 & -0.027 & 0.758 & 0.652 & 72.544 & -2.741 \end{bmatrix}$$

$$B_c=\begin{bmatrix} 0.147 & -0.111 & 0.650 & -0.364 & -1.182 & 0.928 \end{bmatrix}^T$$

$$C_c=\begin{bmatrix} -0.463 & -0.594 & 0.612 & 0.612 & 0.234 & 0.103 \\ -0.845 & -1.086 & 0.335 & 0.356 & -0.295 & -0.154 \\ -1.098 & -1.393 & -0.432 & -0.375 & 0.092 & 0.046 \end{bmatrix}$$

$$D_c=\begin{bmatrix} 0.000 & 0.001 & 0.028 \end{bmatrix}^T$$

$$M_c=\begin{bmatrix} 29.474 & -1.892 & 0.317 \\ -1.892 & 26.302 & -0.467 \\ 0.317 & -0.467 & 35.019 \end{bmatrix} \text{ kg}$$

$$C=\begin{bmatrix} 88.533 & -48.837 & 2.954 \\ -48.837 & 84.950 & -40.885 \\ 2.954 & -40.885 & 38.162 \end{bmatrix} \text{ N} \cdot \text{s/m}$$

$$K=\begin{bmatrix} 100.863 & -53.634 & 2.122 \\ -53.634 & 95.698 & -46.066 \\ 2.122 & -46.066 & 44.553 \end{bmatrix} \text{ kN/m}$$